

The metallicity of K giant stars along the Sagittarius streams

Hong-Bo Ren¹, Wei-Bin Shi^{1,2}, Xu Zhang¹, Yan-Ke Tang³, Yong Zhang⁴, Yong-Hui Hou⁴ and
Yue-Fei Wang⁴

¹ Shandong Provincial Key Laboratory of Optical Astronomy and Solar-Terrestrial Environment, School of Space Science and Physics, Shandong University at Weihai, Weihai 264209, China; swb@sdu.edu.cn

² Research School of Astronomy and Astrophysics, The Australian National University, Weston Creek, ACT 2611, Australia

³ College of Physics and Electronic Information, Dezhou University, Dezhou 253023, China

⁴ Nanjing Institute of Astronomical Optics & Technology, National Astronomical Observatories, Chinese Academy of Sciences, Nanjing 210042, China

Received 2016 August 31; accepted 2017 April 29

Abstract The Large Sky-Area Multi-Object Fiber Spectroscopic Telescope (LAMOST) Data Release 3 provided 341 691 K giant stars with stellar parameters. Based on the models of Law & Majewski, we identified 252 K giant stars in the leading stream associated with the Sagittarius (Sgr) dwarf galaxy. We obtained 132 K giant stars belonging to the trailing arm of Sgr using the model of Belokurov et al. We studied the metallicity distribution of member stars along the streams and found a flat gradient in the first wrap of the leading stream, $-(0.88 \pm 0.3) \times 10^{-3} \text{ dex}/(^{\circ})$ in the second wrap of the leading stream and $-(1.2 \pm 0.3) \times 10^{-3} \text{ dex}/(^{\circ})$ in the first wrap of the trailing stream. Moreover, we obtained a combined metallicity gradient with our sample and data from the literature. We also analyzed the properties of an overdensity, which is located in the leading stream of the Sgr.

Key words: Galaxy: halo — galaxies: individual (Sagittarius) — stars: K giant-branch

1 INTRODUCTION

In the past decades, many dwarf galaxies have been discovered (Belokurov et al. 2006; Newberg et al. 2009, etc). The Sagittarius (Sgr) dwarf galaxy is the most famous one, which was discovered by Ibata et al. (1994). The Sloan Digital Sky Survey (SDSS) mapped the Sgr stream over 360° on the sky (Koposov et al. 2012; Belokurov et al. 2006). In the current theory of hierarchical structure formation, the Milky Way has gained a large fraction of its mass from accretion of a large number of low-mass satellite galaxies. The Sgr streams are disrupted by the gravitational force of the Galaxy. As the satellites are completely or partially disrupted, stars from different satellites mix together and become members of the diffuse stellar halo of the Galaxy (Chen et al. 2014). So, studying the metallicity of Sgr stars is a method to learn about the evolution of the Milky Way.

Many works about Sgr stars have been done. Law & Majewski (2010) presented a new N-body model for

the tidal disruption of the Sgr dwarf galaxy that is capable of simultaneously satisfying the majority of angular position, distance and radial velocity constraints imposed by current wide-field surveys of its dynamically young tidal debris streams. Using a variety of stellar tracers, Belokurov et al. (2014) presented new Sgr detections, accurate distances and line-of-sight velocities that together help to shed new light on the puzzle of Sgr tails. Shi et al. (2012) identified 556 red horizontal branch (RHB) stars in the Sgr streams and analyzed their metallicity distribution. They found a metallicity gradient of $-(1.8 \pm 0.3) \times 10^{-3} \text{ dex}/(^{\circ})$ in trailing arm 1 and $-(1.5 \pm 0.4) \times 10^{-3} \text{ dex}/(^{\circ})$ in leading arm 1. Li et al. (2016) confirmed at least two more substructures near the Sgr leading stream using M giant stars identified by the Large Sky-Area Multi-Object Fiber Spectroscopic Telescope (LAMOST): one is a metal poor substructure in which $[\text{Fe}/\text{H}]$ is between -0.75 dex and -1.20 dex with distances as close as 10 kpc; the other is similar to the North Galactic Cap group detected by Chou et al. (2007).

Chou et al. (2007) identified M giants and obtained a significant metallicity gradient, which showed the [Fe/H] value decreasing from -0.4 dex to -1.1 dex in the leading stream.

K giant stars are excellent tracers for studying Sgr streams because of their bright absolute magnitude. In addition, the LAMOST project (Cui et al. 2012; Luo et al. 2012; Zhao et al. 2012; Deng et al. 2012; Wang et al. 1996; Su & Cui 2004) has identified a large number of K giant stars with relatively accurate parameters (i.e., radial velocities and metallicities) across a wide sky-area. We obtain the data on LAMOST Data Release 3 (DR3) K giant stars from the first author of Liu et al. (2014). Liu et al. (2014) implemented a support vector machine classifier to select K giant stars from the LAMOST survey using their spectral line features, and they applied a Bayesian method to estimate the distance for K giant stars based on metallicity and 2MASS photometry. They concluded that the accuracy of distance estimation depends on the accuracy of metallicity, and systematic bias of the estimated metallicity may induce a systematic bias in estimated distance.

The paper is organized as follows. We present the method to select sample stars in Section 2 and describe the metallicity gradient in Section 3. A discussion is given in Section 4. Finally, we draw conclusions in Section 5.

2 SAMPLE SELECTION

2.1 Sample Selection in Leading Stream

Law & Majewski (2010) provided a Sgr model that has 10^5 points with angular position, distance and radial velocity. By using the model of Law & Majewski (2010), we selected K giant samples belonging to the leading Sgr stream.

First, we obtained 141 561 stars after a right ascension - declination (RA-Dec) cut from 341 691 K giant stars. Second, we selected the stars belonging to the leading arm with a Λ_{\odot} -Distance map (Λ_{\odot} represents the Sgr longitude scale along the orbital plane), which divided the leading stream of Sgr into two parts, leading arm 1 and leading arm 2. (The first and the second wrap of the Law & Majewski (2010) model is denoted by arms 1 and 2, respectively.) We obtained 828 and 1029 K giant stars located in leading arm 1 and leading arm 2, respectively. Third, using the Λ_{\odot} - V_{gsr} map of Law & Majewski (2010), we separated stars in the Sgr streams from Galactic stars. We regard stars as Galactic that agree with the RA-Dec and Λ_{\odot} -Distance cuts but do not satisfy the velocity criteria. We omit overlapping stars and

finally obtain 122 in leading arm 1 and 130 stars in leading arm 2. In Figure 1 we show the selected samples in Λ_{\odot} -Distance and Λ_{\odot} - V_{gsr} maps.

In order to reduce contamination from Galactic halo stars, we omit stars with metallicity [Fe/H] < -2.0 dex. We know that stars from streams are more metal rich than halo stars and metal-poor stars more likely come from the Galactic halo.

2.2 Sample Selection in Trailing Stream

Belokurov et al. (2014) present new Sgr debris detections, accurate distances and line-of-sight velocities that together help provide new information on the structures of the Sgr tails. They give a Λ_{\odot} -Distance map and Λ_{\odot} - V_{gsr} map based on Sloan Digital Sky Survey (SDSS) data. Belokurov et al. (2014) demonstrate that the kinematics of the leading tail is consistent with the model of Law & Majewski (2010). In the trailing stream, they give a $\tilde{\Lambda}_{\odot}$ -Distance map and $\tilde{\Lambda}_{\odot}$ - V_{gsr} map in the range $110^{\circ} < \tilde{\Lambda}_{\odot} < 300^{\circ}$, but there is a significant discrepancy in the part $\tilde{\Lambda}_{\odot} < 210^{\circ}$, where $\tilde{\Lambda}_{\odot} = 360^{\circ} - \Lambda_{\odot}$ (see figs. 6 and 11 in Belokurov et al. 2014).

Using the data of Belokurov et al. (2014), we fit equations corresponding to Λ_{\odot} -Distance and Λ_{\odot} - V_{gsr} for the trailing arm in the range $80^{\circ} < \Lambda_{\odot} < 220^{\circ}$. These equations are

$$\begin{aligned} \text{Distance} = & -3.663 \times 10^{-7} \times \Lambda_{\odot}^4 + 1.22 \times 10^{-5} \\ & \times \Lambda_{\odot}^3 + 0.04368 \times \Lambda_{\odot}^2 - 7.756 \\ & \times \Lambda_{\odot} + 385.147, \end{aligned} \quad (1)$$

$$\begin{aligned} V_{\text{gsr}} = & -2.354 \times 10^{-6} \times \Lambda_{\odot}^4 + 1.28 \times 10^{-3} \\ & \times \Lambda_{\odot}^3 - 0.2148 \times \Lambda_{\odot}^2 + 11.54 \\ & \times \Lambda_{\odot} - 156.159. \end{aligned} \quad (2)$$

We include stars within 20 kpc of the center line in distance and within 40 km s^{-1} in V_{gsr} (Law & Majewski 2010). The fitted center line and boundaries are shown in Figure 2.

Using the model of Belokurov et al. (2014), we selected the K giant samples belonging to the trailing stream of Sgr. We obtained 141 561 K giant stars after the RA-Dec cut. We use the Λ_{\odot} -Distance map and Λ_{\odot} - V_{gsr} map of Belokurov et al. (2014) to select the sample belonging to the trailing stream (see Fig. 2) and we obtained 206 and 132 stars after the Λ_{\odot} -Distance and Λ_{\odot} - V_{gsr} cuts, respectively. Note that in the coordinates defined by Law & Majewski (2010), the leading arm from core to tail corresponds to Λ_{\odot} from 360° to 0° , while in the trailing arm it corresponds to Λ_{\odot} from 0° to 360° .

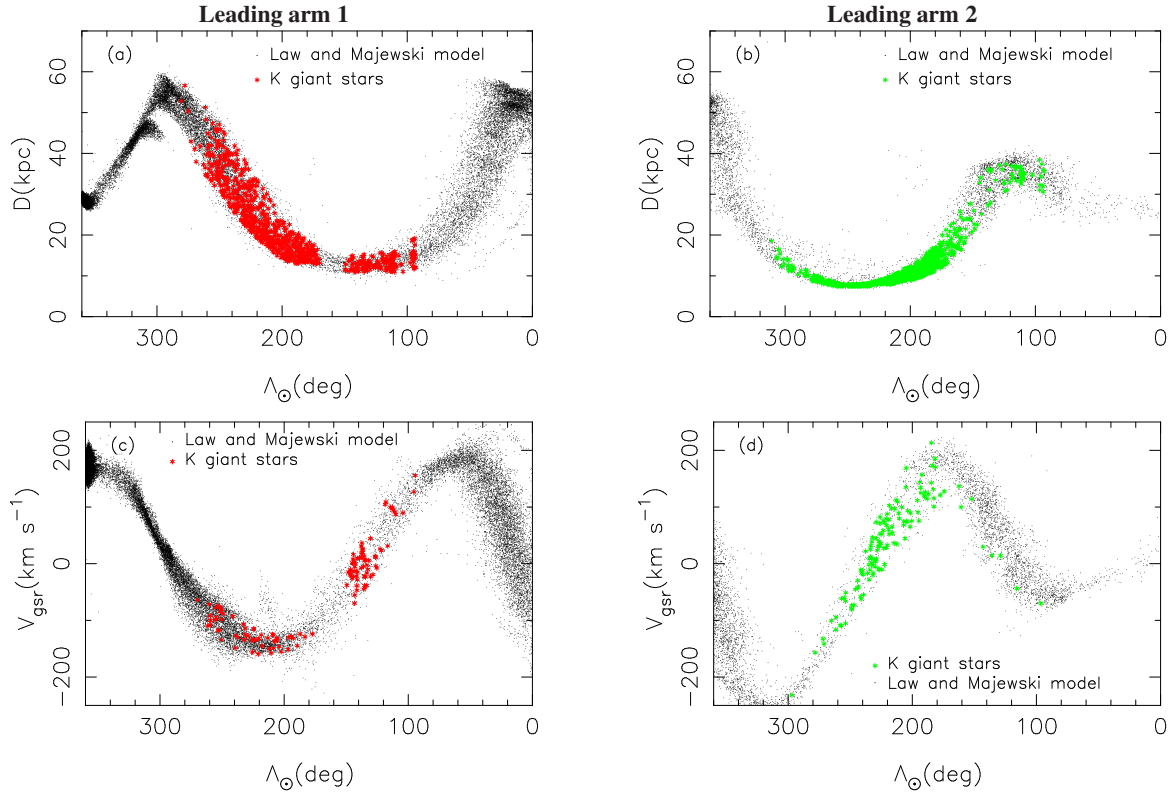


Fig. 1 Using the model of Law & Majewski (2010), we selected K giant stars located in leading arms. The black points represent the model of Law & Majewski (2010). The red points represent the K giant samples in leading arm 1 and the green points represent the K giant samples in leading arm 2. The *upper panels* show the Λ_{\odot} -Distance maps and the *lower panels* show the Λ_{\odot} - V_{gsr} maps.

We display the position of the sample in Cartesian coordinates in Figure 3 and show the first ten sample stars in Table 1 and provide the whole table containing our Sgr sample in an electronic version.

In Table 1 we list the parameters as follows: star identification; RA; Dec; [Fe/H]; distance; V_{gsr} ; Λ_{\odot} ; X_{GC} ; Y_{GC} ; Z_{GC} and mark (L1, L2 and T1 mean leading arm 1, leading arm 2 and trailing arm 1, respectively).

3 RESULTS

3.1 The Metallicity Gradient Along the Leading and Trailing Streams

3.1.1 The metallicity gradients of K giant stars

To study the metallicity of the leading and trailing streams, a linear relationship is shown between metallicity and longitude scale in the orbital plane of Sgr.

Figure 4 shows the Λ_{\odot} -[Fe/H] map of K giant stars in Sgr streams. In Figure 4, the upper panels show the individual points of the K giant stars; the lower panels present the median of individual points with a bin size of ~ 40 degrees in the leading stream and ~ 20 degrees in the trailing stream. We find a flat gradient along

leading arm 1, which agrees with Hyde et al. (2015) and Zhang et al. (2017). Moreover, we obtain gradients of $-(0.88 \pm 0.3) \times 10^{-3} \text{dex}/(^{\circ})$ and $-(1.2 \pm 0.3) \times 10^{-3} \text{dex}/(^{\circ})$ along leading arm 2 and the trailing stream, respectively. In the trailing arm and in leading arm 2, the metallicity of K giant stars decreases as a function of distance from the core. This is consistent with the evolution theory of Sgr streams in which stars in ancient wraps are more metal-poor than stars in new wraps. This also agrees with results from Shi et al. (2012); Zhang et al. (2017); Hyde et al. (2015); Yanny et al. (2009); Keller et al. (2010).

3.1.2 Combined metallicity gradients

The distance of SDSS RHB stars is calculated using the absolute magnitude-metallicity relation (Chen et al. 2009). The distance of LAMOST K giant stars is derived with a Bayesian method and the distance is a function of magnitude, color index and metallicity (Liu et al. 2014). Liu et al. (2014) cross-matched LAMOST data and SDSS DR9 data and show that LAMOST [Fe/H] has a similar trend with smaller bias and dispersion. So, it is reasonable to compare the metallicity gradient of

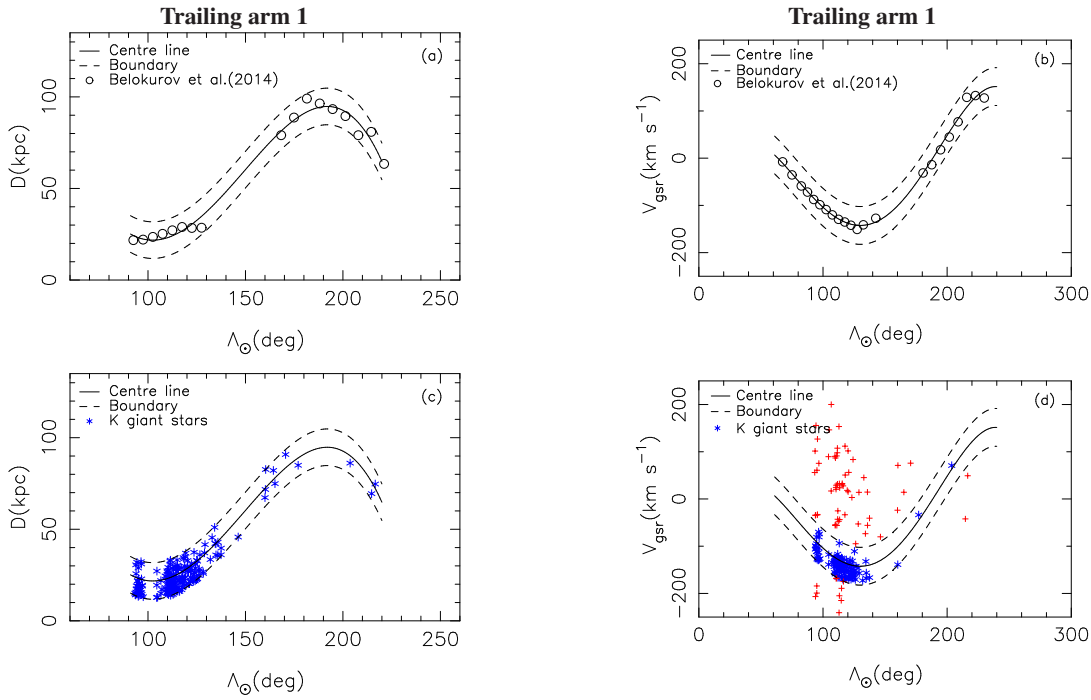


Fig. 2 *Left panels:* The Λ_{\odot} -Distance map of the trailing arm. *Right panels:* The Λ_{\odot} - V_{gsr} map of the trailing arm. *Upper panels:* We fit the lines with the data of the trailing stream in Belokurov et al. (2014). The circles represent the data of Belokurov et al. (2014). The solid lines and dashed lines represent the center-lines and boundaries respectively. 20 kpc and 40 km s^{-1} from the center line define the boundaries in Λ_{\odot} -Distance and Λ_{\odot} - V_{gsr} , respectively. *Lower panels:* Using the model of Belokurov et al. (2014), we selected K giant stars located in the Λ_{\odot} -Distance and Λ_{\odot} - V_{gsr} map. The blue asterisks represent K giants belonging to the trailing stream and the red pluses indicate the halo stars.

Table 1 List of 384 K Giant Stars in Sgr Streams

lmjd-spjd-fiber	RA	Dec	[Fe/H]	D	V_{gsr}	Λ_{\odot}	X_{GC}	Y_{GC}	Z_{GC}	Mark
55861-8-180	60.788	27.527	-1.011	13.038	-69.727	143.245	20.04	2.80	-4.12	L1
55862-2-109	59.295	26.216	-1.135	12.027	-46.854	141.424	18.98	2.56	-4.17	L1
55915-9-85	28.667	3.910	-1.630	12.747	89.559	104.462	14.36	3.45	-10.47	L1
55918-8-148	55.616	4.786	-1.695	14.877	-19.315	128.394	19.75	-0.38	-9.09	L1
55949-5-179	60.793	28.159	-1.044	14.909	3.646	143.544	21.78	3.32	-4.60	L1
56198-3-88	43.674	-7.396	-1.508	11.076	94.732	111.886	14.37	-0.51	-9.02	L1
56212-5-70	55.615	23.394	-1.107	9.979	10.726	137.076	16.80	2.15	-4.15	L1
56213-12-50	39.188	5.511	-1.400	12.095	99.512	114.392	15.72	2.09	-9.05	L1
56217-6-127	57.166	-2.881	-1.587	10.381	-3.765	126.145	15.66	-1.49	-6.81	L1
56217-6-162	57.358	-3.188	-1.785	10.217	11.819	126.170	15.53	-1.53	-6.71	L1

Note: The distances are derived by a Bayesian method (Liu et al. 2014). This table is available in its entirety in a machine-readable form in the online version of the journal (http://www.raa-journal.org/docs/Supp/ms2016_0187table1.dat). A portion is shown here for guidance regarding its form and content.

LAMOST K giant stars with that of SDSS RHB stars. In this work, the analysis of K giant stars produces the main results. We tentatively give the combined gradient and do a comparison.

In Figure 5, we compare our metallicity gradient with that of Shi et al. (2012). Our work and that of Shi et al. (2012) are shown with solid and dashed lines, respectively. Our gradient is very similar to that of Shi et al. (2012) in trailing arm 1. But our gradient is smaller than

that of Shi et al. (2012) in leading arm 1, which means the metallicity of K giants decreases more slowly in leading arm 1. We give a combined metallicity gradient by fitting the median data of our K giant stars and the RHB stars in the leading stream. We obtain a combined metallicity gradient of $-(1.2 \pm 0.3) \times 10^{-3} \text{dex}/(^{\circ})$ in leading arm 1 and $-(0.63 \pm 0.3) \times 10^{-3} \text{dex}/(^{\circ})$ in leading arm 2. We use our K giant stars and the samples of Shi et al. (2012), Chou et al. (2007), Monaco et al. (2005), Keller et al.

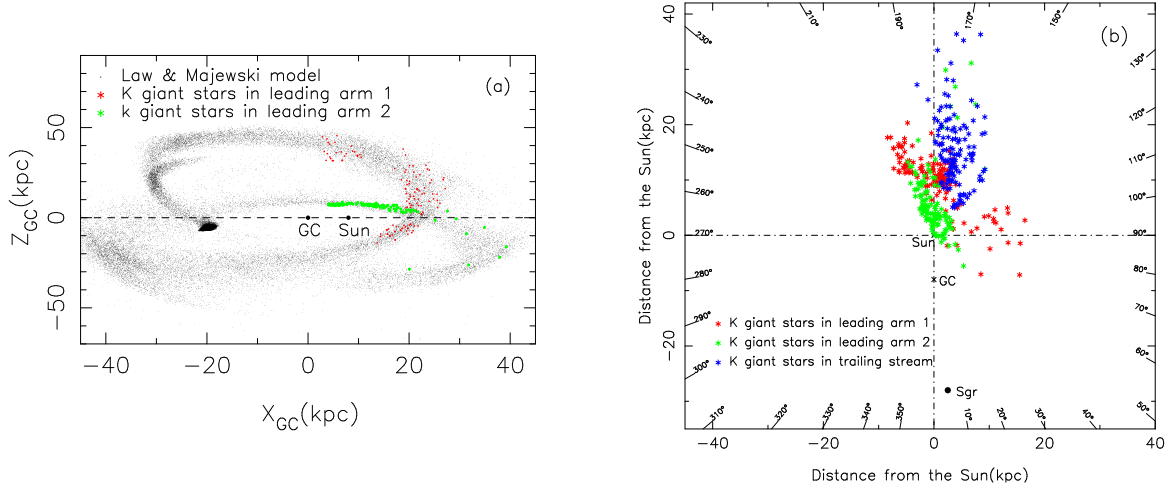


Fig. 3 Red stars, green stars and blue stars show K giant stars in leading arm 1, in leading arm 2 and in the trailing stream, respectively. *Left panel*: K giant stars are shown in the Cartesian Galactocentric plane. The Galactic plane (*dashed line*) and the positions of the Sun and the Galactic center (GC) are also marked for reference. The black points represent the leading stream of Law & Majewski (2010). *Right panel*: spatial distribution of target stars in the debris stream of Sgr projected in Galactic longitude.

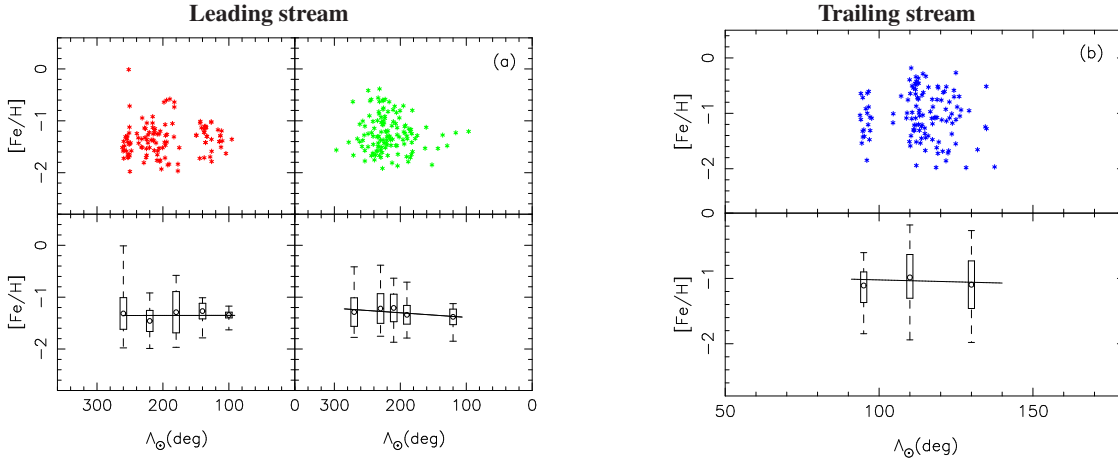


Fig. 4 The metallicity of K giant stars in the Sgr streams expressed as a Λ_{\odot} -[Fe/H] map. *Left panel*: red stars and green stars show K giant stars in leading arm 1 and in leading arm 2, respectively. *Right panel*: [Fe/H] as a function of angular distance along the trailing stream. The upper panel shows the individual points. In the lower panel, the distribution of [Fe/H] in each sample is displayed as a box plot in which the circle represents the median, and the boxed region spans the first to third quartiles. The solid line shows the result of a least-squares linear fit to the median data.

Table 2 List of Trailing Stream Data in the Literature

Stars	Number	Literature
RHB stars	327	Shi et al. (2012)
M giant stars	6	Chou et al. (2007)
RGB stars	19	Monaco et al. (2005)
RGB stars	12	Monaco et al. (2007)
M giant stars	11	Keller et al. (2007)

(2010) and Monaco et al. (2007), see Table 2, to generate a metallicity gradient that is more widespread, which is $-(2.0 \pm 0.4) \times 10^{-3} \text{dex}/(^{\circ})$ in trailing arm 1.

In Figure 5, the red lines show the combined metallicity gradient of Sgr streams.

3.2 An Overdensity in Leading Arm 2

In the left panel of Figure 6 we show the distribution of K giant stars, which agrees with the Λ_{\odot} -Distance cut near leading arm 2. We can see that there is an overdensity at $90^{\circ} < \Lambda_{\odot} < 140^{\circ}$ and $-90^{\circ} < V_{\text{gsr}} < -200^{\circ}$. For further identification, we plot the RHB stars of Shi et al. (2012) in a Λ_{\odot} - V_{gsr} map (right panel of Fig. 6). Fortunately, there is a clear overdensity of RHB stars

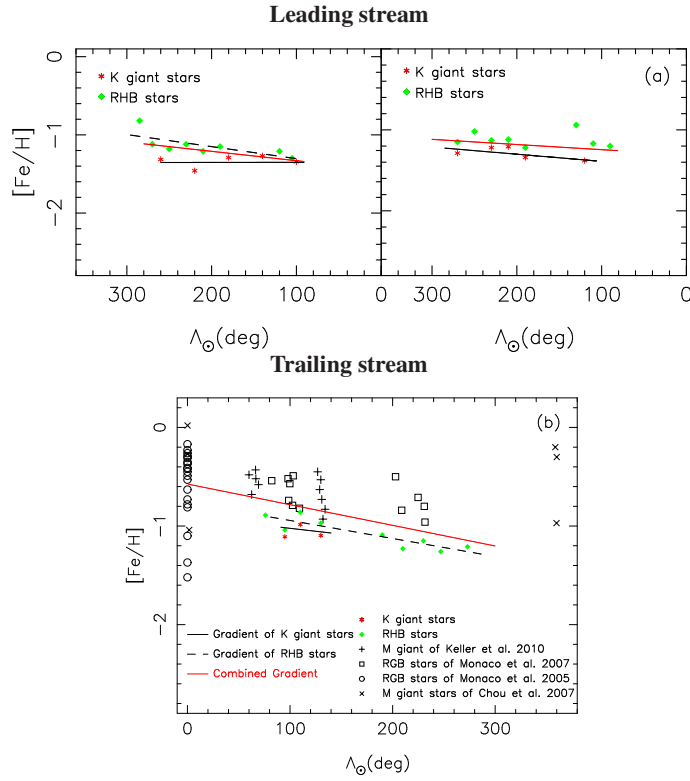


Fig. 5 *Upper panel:* The combined metallicity gradient along the leading stream; left panel and right panel indicate leading arm 1 and in leading arm 2, respectively. The black solid line shows the metallicity gradient of K giant stars, the black dashed line indicates the metallicity gradient of Shi et al. (2012) and the red line indicates the combined metallicity gradient. The red stars show the metallicity median of our data. The green diamonds show the metallicity median of Shi et al. (2012). *Lower panel:* The combined metallicity gradient is fitted with all data along the trailing stream. The pluses, hollow squares, hollow circles and crosses represent the stars from Keller et al. (2010), Monaco et al. (2007), Monaco et al. (2005) and Chou et al. (2007), respectively.

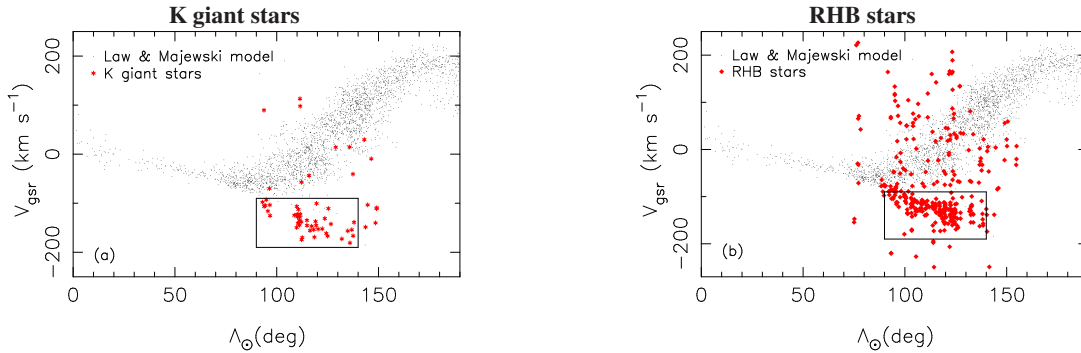


Fig. 6 *Left panel:* The black dots show the model of Law & Majewski (2010) and the red stars show the K giant stars after the Λ_{\odot} -Distance cut. *Right panel:* The red diamonds show the RHB stars after Λ_{\odot} -Distance cut. The box indicates the overdensity.

in a similar position as the K giants. We speculate that this overdensity is a substructure after validating with Newberg et al. (2007). To further determine the possible substructure, we investigate the metallicity distribution of K giant stars and RHB stars in Figure 7. There is a peak in the overdensity between ~ -1.0 dex and ~ -1.2 dex for K giant stars and RHB stars.

We look into the motion of the overdensity relative to the Sgr stream. The overdensity is located inside the stream and moves together with the stream. But the overdensity moves faster than the stars in the stream, so the overdensity will be far away from the original position of the stream. Using the samples in the overdensity and in the stream of Sgr, we perform a Kolmogorov-Smirnov test and obtain a value of ~ 0.9 , which means the over-

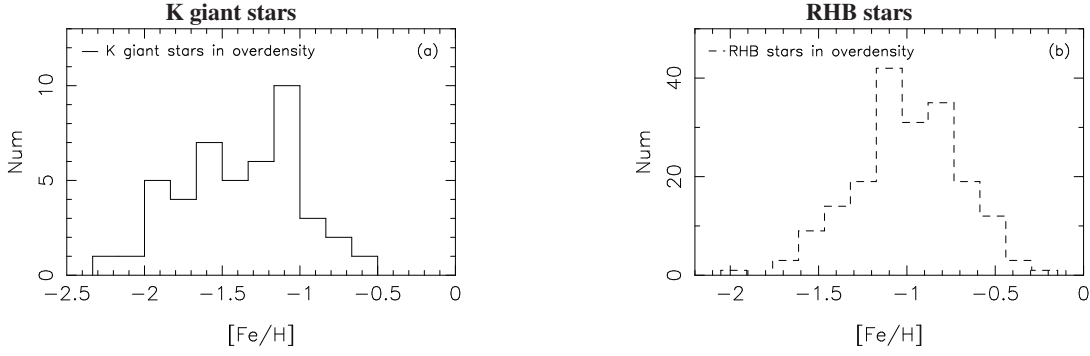


Fig. 7 The metallicity distribution of K giant stars and RHB stars in the overdensity. The solid line indicates K giant stars and the dashed line indicates RHB stars. The peak in the overdensity is at ~ -1.1 dex for both K giant stars and RHB stars.

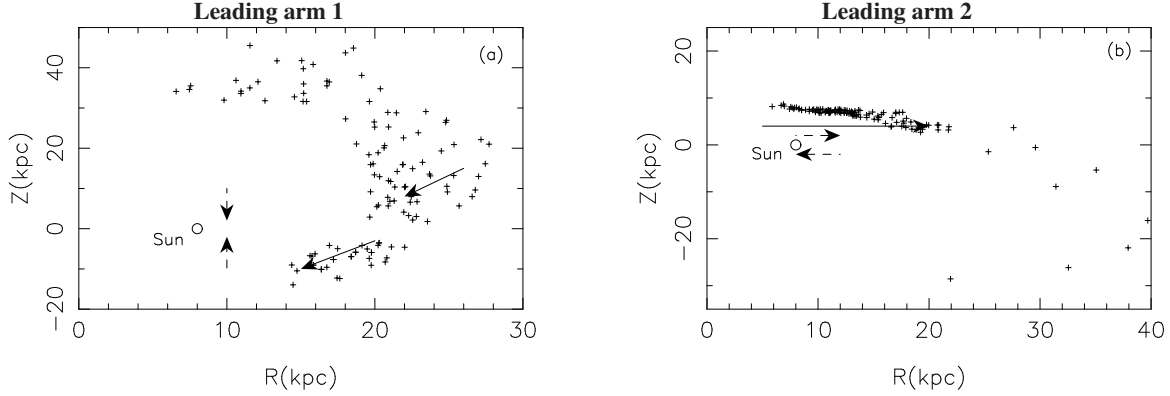


Fig. 8 The solid arrows indicate the kinetic direction of Sgr streams; the dashed arrows indicate the velocity trend of the Galactic disk (Carlin et al. 2013; Williams et al. 2013). *Left panel*: the distribution of K giant stars in leading arm 1. *Right panel*: the distribution of K giant stars in leading arm 2.

density is not the same structure as the leading arm, indicating that the overdensity is likely to be an independent structure.

4 DISCUSSION

4.1 The Contamination of Halo Stars

We estimate the level of contamination in our sample from halo K giant stars in velocity space. We selected samples in the trailing stream after a distance cut with the model of Belokurov et al. (2014) and plot these samples in the lower-right panel of Figure 2 (red pluses indicate halo stars and blue asterisks show stars in the trailing arm). We choose sample stars in the range of $80^\circ < \Lambda_\odot < 140^\circ$ for there is a clear dense band. First, we calculate the average number of stars out of the stream (red pluses in Fig. 2) as an average background of halo stars. Then we determine the number in the stream according to the area of the dense band as the contamination of halo stars and there are ~ 20 halo stars in the trailing stream. The total number of stars is 132 in the

dense band, so the contamination in the trailing stream is $20/132 \sim 15\%$. This contamination may have a small effect on the metallicity gradients, but the effect is within the errors on the metallicity gradients, which indicates that our result is reasonable.

4.2 The Motion of Sgr Streams

We investigate the motion of K giant stars in leading arm 1 and leading arm 2. We compare the kinetic direction of the stream with the velocity trend of the Galactic disk (see fig. 2 of Carlin et al. 2013 and fig. 10 of Williams et al. 2013). From the left panel of Figure 8, we can see that the kinetic direction of the stream is similar to the velocity trend of the Galactic disk above the Galactic plane and the kinetic direction of the stream is opposite to the velocity trend of the Galactic disk below the Galactic plane. From the right panel of Figure 8 we can see that the direction of the Sgr stream is the same as that of the Galactic disk above the Galactic plane.

Furthermore, we need more data to study the kinetic relations of Sgr streams and the Galactic stars in detail.

5 CONCLUSIONS

LAMOST DR3 provided 341 691 K giant stars with stellar parameters. Using the selection criteria of RA-Dec, Λ_{\odot} -Distance and Λ_{\odot} - V_{gsr} , we finally obtained 122, 130 and 132 sample stars in leading arm 1, leading arm 2 and trailing arm 1 respectively.

- (1) We used the K giant sample stars to study the metallicity gradient along the leading and trailing streams of Sgr. We obtained a flat gradient in leading arm 1, a gradient of $-(0.88 \pm 0.3) \times 10^{-3} \text{ dex}/(^{\circ})$ in leading arm 2 and $-(1.2 \pm 0.3) \times 10^{-3} \text{ dex}/(^{\circ})$ in the trailing stream.
- (2) We used K giant sample stars and data provided by the literature to obtain a combined metallicity gradient of $-(1.2 \pm 0.3) \times 10^{-3} \text{ dex}/(^{\circ})$ in leading arm 1, $-(0.63 \pm 0.3) \times 10^{-3} \text{ dex}/(^{\circ})$ in leading arm 2 and $-(2.0 \pm 0.4) \times 10^{-3} \text{ dex}/(^{\circ})$ in the trailing stream.
- (3) We study an overdensity in leading arm 2 and give the distribution of metallicity using our sample and RHB stars provided by Shi et al. (2012).

With the data released by the Gaia spectroscopic survey, we can expect to analyze stars in the Sgr streams for an even larger and more accurate sample.

Acknowledgements We thank the referee for his helpful comments which significantly improved the paper. We thank Chao Liu for his help in providing the data on LAMOST DR3 K giant stars. We thank Kenneth Carrell for his helpful discussion. This work was supported by National Natural Science Foundation of China (Grant Nos. U1631105, 11390371, 11573035, 11233004, 11625313, 11373026, 11303003 and 11673005), the 973 program (No. 2014CB845700) and the Strategic Priority Research Program of the Chinese Academy of Sciences (Grant No. XDB01020300). The Guo Shou Jing Telescope (the Large Sky Area Multi-Object Fiber Spectroscopic Telescope, LAMOST) is a National Major Scientific Project built by the Chinese Academy of Sciences. Funding for the project has been provided by the National Development and Reform Commission. LAMOST is operated and managed by National Astronomical Observatories, Chinese Academy of Sciences.

References

- Belokurov, V., Zucker, D. B., Evans, N. W., et al. 2006, *ApJ*, 642, L137
- Belokurov, V., Koposov, S. E., Evans, N. W., et al. 2014, *MNRAS*, 437, 116
- Carlin, J. L., DeLaunay, J., Newberg, H. J., et al. 2013, *ApJ*, 777, L5
- Chen, Y. Q., Zhao, G., & Zhao, J. K. 2009, *ApJ*, 702, 1336
- Chen, Y. Q., Zhao, G., Carrell, K., et al. 2014, *ApJ*, 795, 52
- Chou, M.-Y., Majewski, S. R., Cunha, K., et al. 2007, *ApJ*, 670, 346
- Cui, X.-Q., Zhao, Y.-H., Chu, Y.-Q., et al. 2012, *RAA (Research in Astronomy and Astrophysics)*, 12, 1197
- Deng, L.-C., Newberg, H. J., Liu, C., et al. 2012, *RAA (Research in Astronomy and Astrophysics)*, 12, 735
- Hyde, E. A., Keller, S., Zucker, D. B., et al. 2015, *ApJ*, 805, 189
- Ibata, R. A., Gilmore, G., & Irwin, M. J. 1994, *Nature*, 370, 194
- Keller, S. C., Schmidt, B. P., Bessell, M. S., et al. 2007, *PASA*, 24, 1
- Keller, S. C., Yong, D., & Da Costa, G. S. 2010, *ApJ*, 720, 940
- Koposov, S. E., Belokurov, V., Evans, N. W., et al. 2012, *ApJ*, 750, 80
- Law, D. R., & Majewski, S. R. 2010, *ApJ*, 714, 229
- Li, J., Liu, C., Carlin, J. L., et al. 2016, *RAA (Research in Astronomy and Astrophysics)*, 16, 125
- Liu, C., Deng, L.-C., Carlin, J. L., et al. 2014, *ApJ*, 790, 110
- Luo, A.-L., Zhang, H.-T., Zhao, Y.-H., et al. 2012, *RAA (Research in Astronomy and Astrophysics)*, 12, 1243
- Monaco, L., Bellazzini, M., Bonifacio, P., et al. 2005, *A&A*, 441, 141
- Monaco, L., Bellazzini, M., Bonifacio, P., et al. 2007, *A&A*, 464, 201
- Newberg, H. J., Yanny, B., Cole, N., et al. 2007, *ApJ*, 668, 221
- Newberg, H. J., Yanny, B., & Willett, B. A. 2009, *ApJ*, 700, L61
- Shi, W. B., Chen, Y. Q., Carrell, K., & Zhao, G. 2012, *ApJ*, 751, 130
- Su, D.-Q., & Cui, X.-Q. 2004, *ChJAA (Chin. J. Astron. Astrophys.)*, 4, 1
- Wang, S.-G., Su, D.-Q., Chu, Y.-Q., Cui, X., & Wang, Y.-N. 1996, *Appl. Opt.*, 35, 5155
- Williams, M. E. K., Steinmetz, M., Binney, J., et al. 2013, *MNRAS*, 436, 101
- Yanny, B., Newberg, H. J., Johnson, J. A., et al. 2009, *ApJ*, 700, 1282
- Zhang, X., Shi, W. B., Chen, Y. Q., et al. 2017, *A&A*, 597, A54
- Zhao, G., Zhao, Y.-H., Chu, Y.-Q., Jing, Y.-P., & Deng, L.-C. 2012, *RAA (Research in Astronomy and Astrophysics)*, 12, 723